24th AIAA Aerodynamic Measurement Technology and Ground Testing Conference **AIAA 2004-2606**
Portland, OR
28 Jun - 1 Jul 2004

MEMS Shear Stress Sensors: Promise and Progress

Mark Sheplak,[1*] Louis Cattafesta,[1†] and Toshi Nishida[2‡]
[1]*Department of Mechanical and Aerospace Engineering*
[2]*Department of Electrical and Computer Engineering*
University of Florida - Gainesville, Florida 32611-6250

and

Catherine B. McGinley[§]
MS170, NASA Langley Research Center
Hampton Virginia, 23681

This paper reviews existing microelectromechanical systems (MEMS)-based shear stress sensors. The promise and progress of MEMS scaling advantages to improve the spatial and temporal resolution and accuracy of shear stress measurement is critically reviewed. The advantages and limitations of existing devices are discussed. Finally, unresolved technical issues are summarized for future sensor development.

I. Introduction

The ability to accurately measure time-resolved wall shear-stress in flows impacts a broad application spectrum that ranges from fundamental scientific research to industrial process control, biomedical applications, etc. It has long been known that macro-scale measurement technology is insufficient to meet the demands of obtaining accurate mean and fluctuating wall shear stress data. In his classic review paper of conventional wall shear-stress measurement techniques, Winter concluded that, *"Of all of the techniques reviewed it is apparent that none can be considered an absolute and reliable standard."*[1] A decade and a half later, Haritonidis came to a similar conclusion, *"No doubt, improved or new instruments will soon appear that extend the rather poor or unreliable capabilities of existing instruments."*[2] In a more recent review papers, Fernholtz et al. reported the uncertainties in mean shears stress for surface fence methods, wall hot wires, wall pulsed wires, and oil-film interferometry to be at least 4% in incompressible flows.[3] Naughton and Sheplak reviewed various oil-film interferometry and liquid crystal techniques with estimated mean shear stress uncertainties of 5% for incompressible flows and 10% for supersonic flows.[4]

To accurately measure time-resolved turbulent wall shear-stress, the sensor must possess sufficient spatial resolution to avoid spatial averaging. In addition, the device must possess large enough measurement bandwidth to avoid excessive low-pass filtering of the data. Both of these requirements must be met to maintain spectral fidelity of the turbulence. For example at high Reynolds numbers, the spatial length scales of interest can be $\mathrm{O}(100\ \mu\mathrm{m})$, and the required bandwidth can be $\mathrm{O}(1\ \mathrm{kHz})$. A simplified scaling analysis indicates that the ratio of the boundary layer thickness δ to the Kolmogorov microscale η scales as $\eta/\delta \sim \mathrm{Re}_\delta^{-3/4}$, where $\mathrm{Re}_\delta = u\delta/\nu$ is the Reynolds number based on δ, u is the typical eddy velocity scale $u/U \sim 10^{-2}$, U is the boundary layer edge velocity, and ν is the kinematic viscosity.[5] Similarly, the ratio of the convective time scale to the Kolmogorov time scale $\Im$

---

[*]Associate Professor, *sheplak@ufl.edu*, Senior Member AIAA.
†Associate Professor, Associate Fellow AIAA.
[‡]Associate Professor.
[§]Aerospace Engineer, Member AIAA.

Mark Sheplak, Louis Cattafesta, Toshikazu Nishida, and Catherine McGinley. "MEMS Shear Stress Sensors: Promise and Progress", 24th AIAA Aerodynamic Measurement Technology and Ground Testing Conference, Fluid Dynamics and Co-located Conferences, https://doi.org/10.2514/6.2004-2606

scales as $\Im u/\delta \sim \mathrm{Re}_\delta^{-1/2}$. Naughton and Sheplak illustrated for that a low-speed air turbulent boundary layer this scaling yields Kolmogorov scales of $\eta \approx 200\,\mu\mathrm{m}$ and $\Im \approx 2\ \mathrm{ms}$.[4] While the viscous wall unit ν/u^* (where $u^* = \sqrt{\tau_w/\rho}$ is the friction velocity, τ_w is the wall shear stress, and ρ is the density) is often used to determine the spatial resolution performance of probes in turbulent boundary layers, the above scaling is sufficient to illustrate the stringent spatial resolution requirements for turbulent flows.[6] In addition, a flat frequency response function is desired for turbulence measurements so that the spectra and statistical moments are accurately estimated. If the required data analysis requires correlation analysis, a zero-phase frequency response function over a wide frequency range is also desirable. Therefore, the characterization of the sensor/compensation system dynamic response is necessary to bound measurement uncertainty for time-resolved data.

Among conventional techniques, Fernholtz et al. points out that only hot-film probes and wall-mounted hot wires offer the potential to provide time-resolved measurements.[3] Yet the uncertainty of their dynamic response — due to heat conduction to the wall, calibration difficulties, flow perturbation due to heating, and nonlinear response due to large fluctuations with respect to the mean (~40%) — has not been quantified.[4] In addition, a single thermal sensor is unable to discern the direction of the wall shear stress, thus limiting their usefulness in separated flows. In summary, the accurate, time-resolved direct measurement of fluctuating wall shear stress has not been realized using conventional sensor technology. As will be illustrated in subsequent sections, the inherent small physical size of microfabricated transducers offers the potential to overcome some of the traditional limiting factors associated with conventional techniques.

Microelectromechanical systems (MEMS) fabrication technology leverages and extends silicon-based integrated circuit fabrication techniques to synthesize miniature engineering systems.[7] This miniaturization technology provides the opportunity to develop sensors possessing performance that greatly exceeds conventional macro-scale fabrication techniques. From the perspective of shear-stress measurement instrumentation, the small physical size and reduced inertance of micro-sensors offers the potential to vastly improve both the temporal and spatial measurement bandwidth, thereby meeting the stringent specifications for time-resolved wall shear stress measurements discussed above.

Realizing the potential performance advantages of developing shear stress sensors via MEMS technology, a number of researchers have presented an assortment of micromachined devices at various stages of technical maturity. Overviews of the operational characteristics and performance of these devices has been presented in two recent review papers.[4,8] This paper updates these reviews with the addition of more recent sensor technology and then examines several unresolved technical issues that must be addressed before these devices can be considered standard, reliable measurement tools possessing quantifiable uncertainties. The next section provides a brief overview of existing MEMS sensors that includes a discussion of the outstanding technical issues of these devices. Finally, the paper offers some conclusions and prospective for future research directions.

II. Existing MEMS Sensors

Wall shear-stress sensors are traditionally classified by measurement method into two distinct groups, direct or indirect techniques.[2] The former directly measure the shear force acting on the model surface. This is typically achieved by employing a "floating element" balance. Indirect techniques require an empirical or theoretical correlation, typically valid for very specific conditions, to relate the measured property to the wall shear stress. The MEMS community has produced a variety of different indirect transduction schemes such as hot-film sensors, micro-optical systems to measure near-wall velocity gradients, and mechanical micro-fences. An overview of these techniques and their respective advantages and disadvantages are presented below.

A. Floating Element Sensors

Direct sensors measure the integrated wall shear force on a floating element of length L_e, width W_e, and thickness t that is flush mounted to the surface as shown in Figure 1. The floating element is suspended over a recessed gap g by mechanical tethers that also serve as restoring springs possessing a stiffness k. The shear stress is then related to the displacement of the element Δ which in turn is measured via a transducer. It is also possible to incorporate the element in a feedback force-rebalance configuration. Numerous macro-scale variations of this device have been developed using conventional manufacturing technology, but the performance of these devices has been historically limited by the following issues:[1]

1. Tradeoff between sensor spatial resolution and the ability to measure small forces
2. Measurement errors associated with sensor misalignment

3. Measurement errors associated with required gaps
4. Measurement errors associated with pressure gradients
5. Cross-axis sensitivity to acceleration and vibration
6. Sensitivity drifts due to thermal-expansion effects

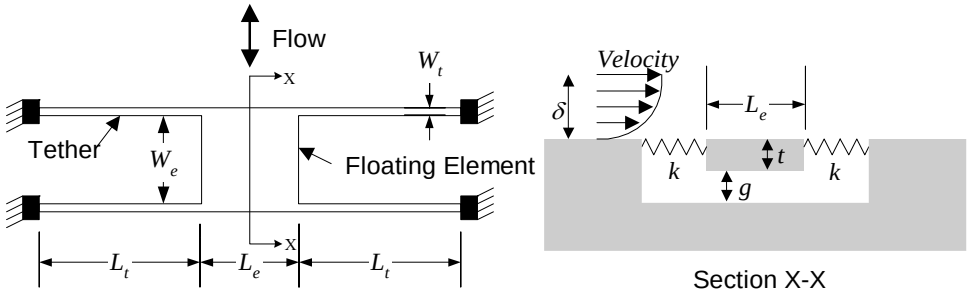

Figure 1 Schematic plan view and cross-section of a typical floating-element sensor.

The scaling advantages of MEMS devices are illustrated by employing a simple analysis of the four-beam tether shown in Figure 1.[4] The ability to fabricate MEMS devices enables the development of thin, low mass, compliant mechanical sensors possessing superior sensitivity-bandwidth products relative to conventional sensors assuming equal compliances. For example, typical conventional floating elements scale as $L_e \sim W_e \sim \mathrm{O}(1\ \mathrm{cm})$ and $t \sim \mathrm{O}(1\ \mathrm{mm})$, while a typical micromachined floating element has $L_e \sim W_e \sim \mathrm{O}(100\ \mu\mathrm{m})$ and $t \sim \mathrm{O}(1\ \mu\mathrm{m})$.[9] In the recent review of existing MEMS floating-element sensors, the following favorable attributes with regards to the limitations listed above were noted.[4]

1. Non-optimized MEMS sensors have already demonstrated minute force detection $\mathrm{O}(0.1\ \mathrm{nN})$, which corresponds to a shear stress resolution $\mathrm{O}(10\ \mathrm{mPa})$, for a sensor area of only $100\ \mu\mathrm{m}\ x\ 100\ \mu\mathrm{m}$.[10]
2. Micromachined shear-stress sensors possess negligible sensor misalignment errors because the floating element, tethers, and the substrate are all monolithically fabricated, not assembled, from the same wafer, but care must be taken in packaging and tunnel installation to avoid such errors.[9]
3. A typical micromachined floating-element sensor possesses gaps and depths $\mathrm{O}(1\mu\mathrm{m})$, which, except at extremely high *Re*, is less than a few viscous wall units and is thus considered to be hydraulically smooth.[11]
4. Micromachined sensors render pressure-gradient induced measurement errors negligible due to approximately a three order-of-magnitude reduction in scale, $t \sim g \sim \mathrm{O}(1\mu\mathrm{m})$ compared to conventional sensors possessing $t \sim g \sim \mathrm{O}(1\mathrm{mm})$.[9]
5. The cross-axis acceleration/vibration sensitivity scales with the element mass, so this sensitivity for MEMS sensors is three-orders of magnitude smaller than for conventional sensors.[10]
6. Micromachined shear-stress sensor silicon die are immune to thermal expansion-induced sensitivity drift because the floating element, the tethers, and the substrate are all monolithically fabricated, but care must be taken in packaging to avoid such errors.[9]

Realizing the scaling advantages of MEMS-based floating element sensors listed above, several researchers have developed various types of micromachined floating-element sensors. The various contributions and corresponding limitations of these devices are summarized below in an effort to reveal progress and challenges in the sensor designs.

Schmidt et al. first developed a micromachined floating-element sensor for shear-stress measurements in a turbulent boundary layer.[9] The device was fabricated using a polyimide/aluminum surface micromachining process and incorporated a differential capacitive scheme to sense the element movement as shown in Figure 3. While this proof-of-concept device demonstrated the potential of micromachined shear-stress sensors, the use of polyimide in a capacitive sensing scheme was problematic. Moisture variations changed the mechanical properties (residual stress) of the polyimide to change due to induced swelling, which led to mechanical sensitivity drift. The air-dielectric interfaces were subjected to charged species accumulation that manifested as drift when detected by the capacitive

plates of the sensor. The high input impedance of the sensor also made it sensitive to electromagnetic noise interference (EMI).

Ng et al. and Goldberg et al. extended the work of Schmidt et al. by developing piezoresistive-based floating-element sensors (Figure 2) for polymer extrusion processing in very high shear stress level application (1.0 kPa to 100 kPa).[12,13] While these sensors were not developed for turbulence measurements, they represented an important contribution in the development cycle because they possessed backside electrical contacts to protect the wire-bonds from the harsh environment. However, this was accomplished using wet-chemical etching techniques that resulted in unacceptably large chip sizes, several millimeters on a side. The elimination of wire bonds is crucial for turbulence measurements to reduce the sensor flow disturbance and the associated measurement uncertainty, in addition to electrically isolating the sensor from the fluid medium.

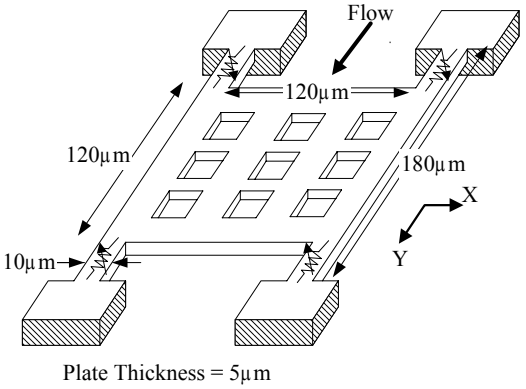

Figure 2 Top-view schematic of an axial piezoresistive floating element sensor developed by Ng el al. and Goldberg et al. [12,13]

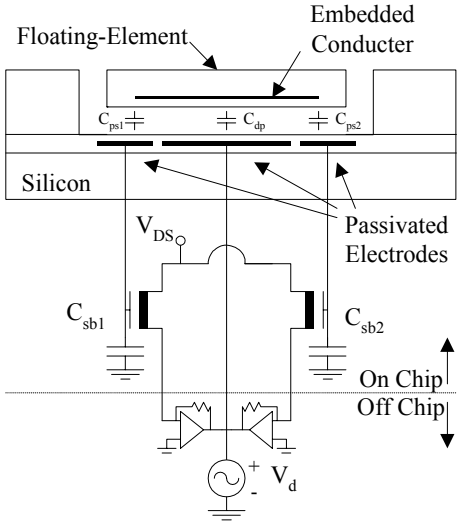

Figure 3 Side-view schematic of a differential capacitance floating element sensor developed by Schmidt el al.[9]

Padmanabhan et al. developed two generations of differential optical-shutter-based floating-element sensors for turbulence measurements.[10,14] As shown in Figure 4, photodiodes were integrated into the substrate under the floating element at the leading and trailing edges of the floating element. A coherent light source illuminated the element from above such that a differential photocurrent (leakage current of a reverse-biased p-n junction) was produced in direct proportion to the lateral displacement of the element and, hence, the shear stress. Static calibrations demonstrated a maximum non-linearity of 1% over four orders of magnitude (1.4 mPa - 10 Pa). The dynamic response was also qualitatively shown to exceed 10 kHz.[10,15] Furthermore, the device was insensitive to environmental effects such as EMI and stray charging when compared to capacitive detection schemes.[9] The differential scheme also demonstrated negligible cross-axis sensitivity to spanwise shear stress, acceleration, and pressure fluctuations. Drawbacks to this sensor include front-side electrical contacts (i.e., a flow disturbance) and the remote mounting of the incident light source from sensor. This separation resulted in unavoidable sensitivity to any mechanical movement of the light source relative to the sensor (tunnel vibration, tunnel expansion, etc.).

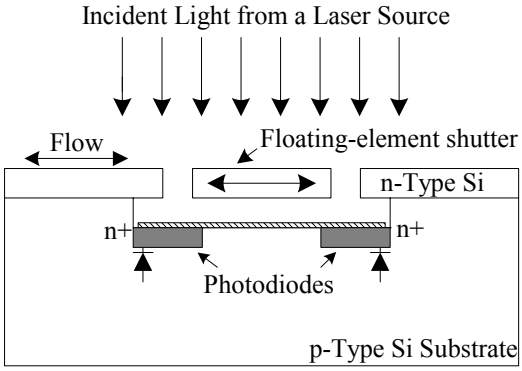

Figure 4 Side-view schematic of the differential optical shutter floating element sensor developed Padmanabhan et al. [10,14]

Pan et al. and Hyman et al. reported a surface-micromachined, force-feedback capacitive design that monolithically integrates the sense, actuate, and control electronics on a single chip.[16,17] A schematic of the comb-finger capacitive design in shown in Figure 6 These devices were shown to be very sensitive over a limited dynamic range, but possessed a nonlinear static response. Additionally, surface micromachined sensors are not flush-mounted by definition.

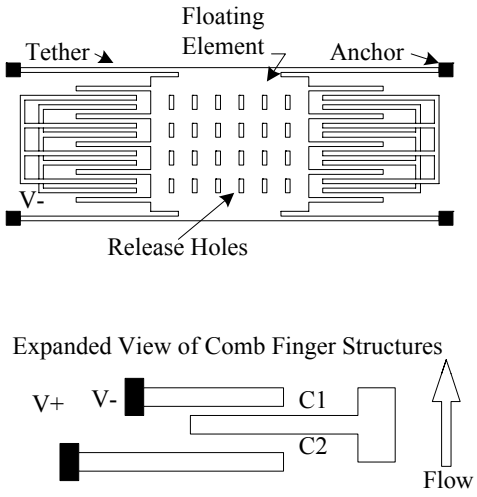

Figure 6 Side-view schematic of a differential capacitance surface micromachined floating element sensor developed by Pan et al. and Hyman et al. [16,17]

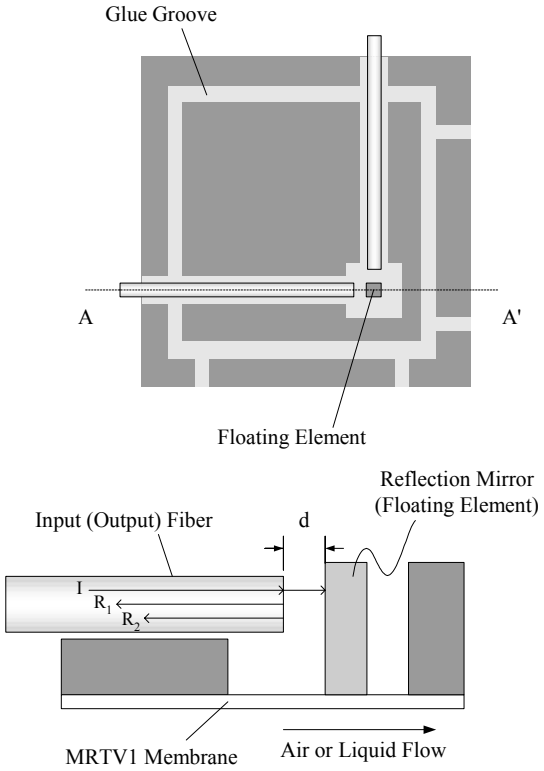

Figure 7 Bottom and side-view schematics of a Faber-Perot based floating element sensor developed by Tseng, and Lin[19]

Zhe et al. reported a cantilever-based floating-element sensor using a capacitive detection scheme.[18] This device differs from the traditional floating element 4-tether structures, by using a cantilever beam with the sensing area located at the end as shown in Figure 5. The authors mainly focused on capacitive sensing and actuation characterization but did not report any shear-stress measurement results.

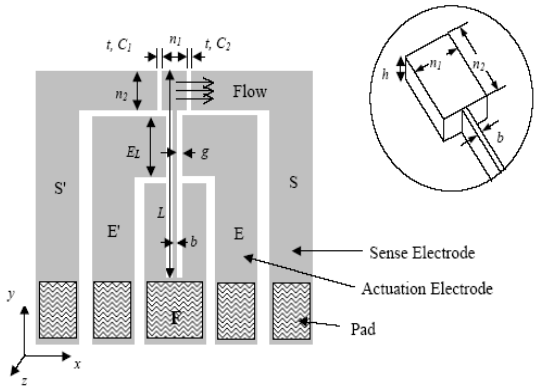

Figure 5 Top-view schematic of a differential capacitance cantilever design floating element sensor developed by Zhe et al. [18]

Tseng and Lin reported a micro-Fabry–Perot interferometer optical fiber-based floating element stress sensor utilizing a flexible membrane and double SU-8 resist structures as a moving micro-mirror.[19] The sensor is fabricated using polymer MEMS-based processes to realize the flexible membrane and double SU-8 resist layers as the sensor structure. As shown in Figure 7, the floating element optical fibers are shielded from the flow by the flexible membrane. Static calibration tests in a flow indicate a maximum detection displacement of the floating element of 10 nm, a sensitivity 0.128 nm/nm (spectral shift/floating element displacement) which corresponds to a shear stress sensitivity of 0.65 Pa/nm with a temperature coefficient of 3.4 nm/K. The bandwidth of this device was not reported. While this device truly represents a flush-mounted design and is immune to EMI, the noise floor of the device is high (2 nm or 1.3 Pa) and, given the mechanical structure, vibration and pressure sensitivity might be an issue.

Horowitz et al. developed a floating-element shear-stress sensor employing an optical Moiré transduction technique.[20,21] The sensor was fabricated using an aligned wafer-bond/thin-back process producing optical gratings on the backside of a floating element and on the top surface of the support wafer (Figure 8). A high-speed, linescan CCD camera measured the resulting Moiré pattern displacement through a 5x optical lens which was imaged via a microscope. The flow disturbance is minimal because the incident and reflected

light comes through the backside of the Pyrex wafer. This scheme also possesses immunity from EMI and transverse element movement due to pressure fluctuations and/or vibrations. Results indicated a mechanical sensitivity of 0.26 μm/Pa, while the Moiré fringe, after the 5x optical amplification, moves by 130 μm/Pa., and exhibited a linear response up to the maximum tested value of 1.3 Pa. Dynamically, the device was found to a have a resonant frequency of 1.76 kHz and a minimum detectable shear stress of 6.2 mPa for a 1 Hz bin centered at 1 kHz. A major limitation of this device consists of the complex imaging system and associated bulky package. The sensor package was constructed for preliminary bench-top characterization using a microscope and requires further development.

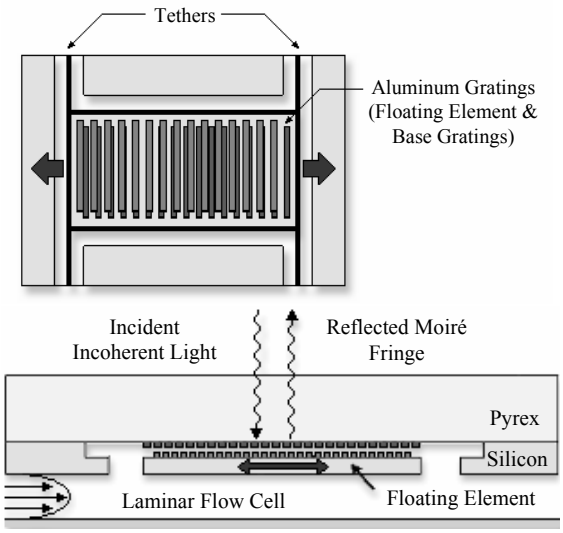

Figure 8 Top- and side-view schematics of a optical Moiré-based floating element sensor developed by Horowitz et al. [20,21]

B. Thermal Sensors

The operating principle of hot-film shear stress sensor is simply the transduction of heat-transfer rate to voltage. Current is passed through a sensor element comprised of a material that possesses desirable temperature-resistance characteristics (i.e., the temperature coefficients of resistivity are large and known). As the temperature of the sensor varies with changes in the flow environment due to convective heat transfer, so does the resistance and, hence, the Joulean heating rate. The typical device structure consists of a thin film sensing element of streamwise length L and spanwise width W deposited on a surface exposed to the flow with the goal of thermally isolating the sensor from the supporting surface (see Figure 9). During operation, the sensing element is heated to a temperature T_s greater than the fluid temperature T_∞, defining the nondimensional thermal overheat ratio

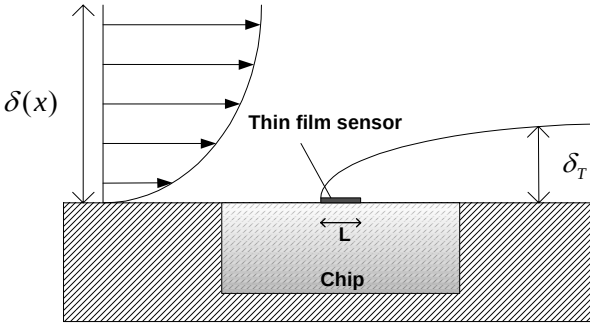

Figure 9 Side-view schematic of a typical thermal sensor.

$$a_T = \frac{T_s - T_\infty}{T_\infty} = \frac{\Delta T}{T_\infty}. \tag{1}$$

This localized heating of the surface generates a thermal boundary layer, $\delta_T(x)$, within the velocity boundary layer, $\delta(x)$. As the temperature of the sensor varies with convective heat transfer changes in the flow environment, so does the resistance and, hence, the Joulean heating rate. The convection of heat from the sensor is measured by monitoring changes in the temperature-dependent resistance of the sensing element given by

$$R_s = R_r\left[1+\alpha\left(T_s - T_r\right)\right], \tag{2}$$

where R_s is the sensor resistance, T_r is a reference temperature corresponding to a sensor reference resistance R_r, and α is the thermal coefficient of resistance (TCR).

The primary difficulty associated with thermal shear-stress sensors is that an empirical correlation is required to relate the measured Joulean heating rate to the wall shear stress. In addition, the dynamic response of the sensor is limited because of its finite thermal inertia, and external compensation is used to extend the measurement bandwidth. Several review articles describe the operating principles and classical modeling of thermal-based shear stress sensors.[1,2,4,8] These reviews point out that all thermal sensors possess reductions in sensitivity and complications in the dynamic response due to the frequency-dependent conductive heat transfer into the supporting structure. This unsteady heat conduction creates a low-frequency roll-off in the gain factor of the frequency response function as well as a corresponding frequency-dependent phase lag.

As stated above, all thermal sensors possess several limitations when attempting to using them for quantitative wall shear stress measurements. Review articles on conventional based thermal sensors list the following limitations:[1,2]

1. Measurement errors associated with mean temperature drift
2. Difficulty in obtaining a unique calibration or relationship between heat transfer and wall shear stress
3. Reduction in sensitivity and complications in the dynamic response due to the frequency-dependent conductive heat transfer into the substrate
4. Flow perturbations due to heat transfer to the flow

Initially, researchers thought that the advantages of silicon micromachined sensors versus conventional devices in terms of improved thermal isolation held the promise of overcoming these limitations (see Naughton and Sheplak for a more complete review[4]). From a device scaling perspective, the combination of micron-scale sensor lengths and improved thermal isolation offer the following performance enhancements over conventional sensors: increased spatial and temporal resolution, higher sensitivity, lower power dissipation, and a potential reduction in the complications due to unsteady heat conduction into the substrate. Realizing this potential, the collaborative efforts of Ho and Tai and their co-workers (see, for example, references 22-26) resulted in the development of a novel polycrystalline silicon-based sensor on a silicon nitride membrane over a vacuum cavity designed to reduce substrate conduction effects (Figure 10). This device design and various iterations represented a significant advancement in thermal shear-stress sensor technology, resulting in improvements in sensitivity, bandwidth, and power consumption over conventional hot-film devices. While these devices have been successfully used for flow control applications,[23] the complete experimental characterization required to extend their use to providing quantitative turbulence data has not been adequately reported. Specifically, experimental verification of the dynamic response, noise floor, pressure sensitivity, thermal disturbance of the flow and thermal drift are important measurements that are needed to fully characterize the performance of any thermal shear stress sensor.

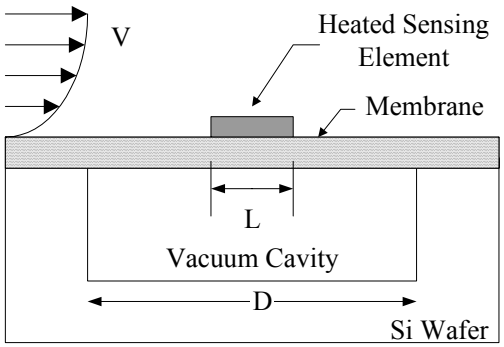

Figure 10 Side-view schematic of a typical vacuum cavity thermal sensor.

The current authors have also investigated vacuum cavity sensor configurations that extended the work of Ho and Tai via an improved design in terms of sensing element material (platinum) and a novel fabrication process to yield improvements in thermal isolation. The main goal of our research was to rigorously assess the viability of performing quantitative measurements via comprehensive numerical and experimental studies.[27,28,29] We found that while these device designs and various iterations resulted in improvements in sensitivity, bandwidth, and power consumption versus conventional hot-film devices, the fundamental limitations listed above could not be overcome. Additional research groups have also examined vacuum cavity sensors, but have also not overcome these limitations.[4,30,31] Specifically, we found the following issues corresponding to the above limitations:

1. Sensitivity associated with mean temperature drift is an issue and is not easily corrected.
2. We were unable to obtain a unique calibration between heat transfer and wall shear stress for a laminar flow calibration cell and turbulent boundary layer given an identical mean wall shear stress.
3. The dynamic response possesses two time constants, indicating that there is still significant frequency dependent conductive heat transfer into the substrate/membrane in vacuum cavity sensors.[27,28]
4. Flow perturbations due to heat transfer from the sensor to the flow can contribute additional errors of 5% or greater.[29]

To use thermal shear stress sensors in large wind-tunnel production-type testing or even in the small scale laboratory wind tunnel, the sensors must be correctable for ambient temperature changes. For many years, conventional thermal shear stress sensors (i.e., hot films) have been used to provide qualitative descriptions of the shear stress behavior on wind tunnel models. Useful quantitative values, however, such as the locations of transition, separation, and reattachment have also been inferred from these measurements.[32] Only in laboratory

settings, where the temperature can be tightly controlled, can we hope to obtain quantitative values of the shear stress with thermal based sensors. In large facilities, however, temperature changes can be on the order of 10 ºC.[32] Also, in typical large wind tunnel tests the sensors are often placed on the surface of a model that experiences complex flow phenomena and an in-situ calibration of the device is generally impossible.

The behavior of conventional hot films has been studied over the years, but only a limited amount of attention has been paid to the temperature problem. For example, the early work by Bellhouse and Shultz discussed the sensitivity to temperature changes. They remarked that even a change in temperature of 0.1 ºC was significant.[34] The theory they presented indicated that conventional films are primarily sensitive to the difference between the film temperature and the temperature of the surroundings. Therefore, to study the thermal sensitivity of the films they simply altered the film temperature instead of the flow temperature. For changes in temperature up to 4 ºC they proposed using

$$\tau_w^{1/3} = A\left(\frac{i^2 R_r}{T_s - T_\infty}\right) + B, \tag{3}$$

where A and B are constants, and the changes in $(T_s - T_\infty)$ were then accounted for in the term $(T_s - T_\infty)$. For temperatures greater than 4 ºC, they suggested that A and B be treated as functions of the temperature difference $(T_s - T_\infty)$ and a calibration versus temperature be performed. Data were presented over various film temperatures and no attempt was made to determine that corresponding changes in the flow temperature, holding the film temperature constant, would affect the calibrations of the sensors in the same manner.

Mathews also examined the temperature sensitivity of conventional films.[35] He used a well-insulated film and noted that the insulated film took a long time to dissipate its heat when turned off and that this could result in unrepeatable calibrations if sufficient time was not allowed for the sensor to return to equilibrium. He tested for temperature sensitivity in the same manner as Bellhouse by changing the temperature of the film, in his case over a range of 60 ºC. Examining the effect of correcting for changes in the temperature dependent fluid properties he concluded that fluid property variations were not primarily responsible for the effects of sensor temperature changes on sensor performance. He attempted to correct for the effects of the temperature changes using several methods centered on the difference between the wire temperature and a nearby surface temperature measurement, but he did not find any method capable of collapsing the data.

Cousteix and Jullien tested a wire mounted flush with the surface and embedded in an insulating material.[36] They found that a 1.4 ºC temperature change could result in an error of 35% in the shear stress. In order to study the effect of temperature changes, they varied the wire temperature and the air temperature. Their data suggest that the effect of changing one is similar to the other, but no correction method was demonstrated.

Due to the complicated heat transfer problem that exists for conventional hot films (primarily due to conduction into the substrate) it is not surprising that no robust correction method has emerged. If we look at the less complicated heat transfer problem of the hot-wire anemometer we see that simply reducing the conduction into the substrate will not guarantee a solution. The hot-wire anemometer has been studied far more extensively than the hot film, but temperature corrections still remain a difficulty and no established method is recognized. The primary methods to account for the effects of ambient temperature changes on hot wires are maintaining constant overheat ratio, analytically correcting for the temperature change based on heat transfer relationships, and direct calibration of the probe for changes in temperature and velocity.[37-41] That researchers today still resort to directly calibrating the wire for temperature is an indication of their frustration with the lack of robustness of the other methods. Given the record for conventional hot films and hot wires, with respect to corrections for temperature changes, the MEMS-based thermal shear-stress community has a clear challenge ahead of it.

Only a few authors have attempted to correct MEMS-based thermal shear stress sensors for changes in the ambient temperature. Nagaoka et al. used a polysilicon sensor on a nitride diaphragm with a 2 μm deep cavity underneath the diaphragm.[42] They applied a software correction to the voltage output that was based on the measured ambient temperature change. No details of the correction method were provided and no calibration versus temperature was shown. Jiang et al. used a similar sensor and proposed electronic compensation for ambient temperature changes using a nearby film as a temperature sensor.[43] They presented corrected and uncorrected data over a temperature range of 0.7 ºC. The data demonstrate that the output voltage, over that temperature range, was adjusted so that it was far less sensitive to changes in the temperature. Later, Huang et al., using the same type of sensor, anemometer, and compensation method, presented results over a similar temperature range.[44] They too showed data that indicated that the temperature sensitivity of the output of the anemometer was reduced. However, in this instance the compensation resulted in an increase in the scatter of the data. While a reduction in the sensitivity of the voltage output to changes in temperature certainly seems like an improvement, no repeatability in

shear stress measurements over a change in temperature was demonstrated. Ruedi et al. used similar sensors as above, but different constant temperature anemometers with no temperature compensation.[45] They concluded that if the sensors were allowed time to equilibrate that wall temperature changes were not a problem, but they also stated that changes in flow temperature still remained a problem. They suggested, as others have in the past, that operating the films at a higher overheat ratio would not only increase the sensitivity to shear stress but would also mitigate the temperature sensitivity. Subsequently, however, Ruedi et al. found that operating at a higher overheats (in their case 1.3) affected their ability to measure consistent values of the fluctuating shear stress close to the wall.[46] They then proposed that the films be run at an overheat ratio at or below 1.2 with some type of compensation for the effects of ambient temperature changes.

Using a thermal shear stress sensor made of a platinum element on a silicon nitride membrane with a 10 μm cavity below it and powered by a constant current source, Sheplak et al. varied the overheat ratio to demonstrate the dependence of the sensor output on overheat ratio over a range of shear stress values.[28] The sensitivity of the sensors to changes in shear stress increased with increases in overheat ratio. No attempt was made to correct the data for changes in the overheat ratio. It was pointed out that as the overheat ratio increased there was likely contamination from buoyancy effects from the sensor heating the flow. Appukuttan et al. specifically studied this phenomenon and concluded that induced buoyancy due to sensor heating of the flow can be a factor for these MEMS sensors.[29] Therefore, the idea of operating films at high overheat in order to mitigate the effects of temperature changes might run counter to the desire not to alter the very quantity being measured. It is of interest to note that conventional wall-mounted hot-film sensors typically have thus been run at low overheat ratios.

Lofdahl et al. used micro hot wires located 50 μm to 250 μm above the surface as indicators of shear stress.[47] In an experimental and analytical study of the effects on the micro hot-wire output due to changes in the ambient temperature, they found that the sensitivity of the wire to temperature decreased with increasing τ, increased as the wall was approached, and decreased with an increase in overheat ratio. The experimental data and analytical predictions have the same trends but do not agree quantitatively. They did find that a temperature change on the order of 0.1 ºC resulted in a measurable difference in the shear stress.

A further complicating issue with thermal sensors is the unequal static and dynamic sensitivities due to the unsteady heat conduction into the supporting structure. Since the conjugated conduction/convection heat transfer problem is strongly dependent upon the flow parameters, the dynamic sensitivity cannot be inferred from a steady-state (static) calibration. Thus, an in-situ dynamic calibration is required to determine the frequency response function of a hot-film sensor. This is a fundamental characteristic of hot-film sensors, and any quantitative application of them must address this complexity. Errors associated with this phenomenon corrupt spectral measurements, rms turbulent shear stress levels, and cross-correlation measurements. Unequal static and dynamic sensitivities will also produce errors in the statistical moment estimates. For example, in a study involving conventional hot-film shear stress probes, Alfredsson et al. noted that using the static calibration to reduce dynamic data resulted in a significant under-prediction of the rms turbulent shear stress levels when there was substantial heat conduction to the substrate.[6] Specifically, large variations were reported in the axial turbulent wall shear stress intensity $\tau'_{rms} / \overline{\tau}_w$. Because of the unknown dynamic response of thermal sensors, it is virtually impossible to separate errors in spatial averaging from those due to unsteady heat conduction.

Sheplak et al. have obtained dynamic wall shear stress sensitivities at multiple mean shear stress levels and overheats for a vacuum cavity sensor driven in a constant current mode using an in-situ dynamic calibration technique.[28] This technique provided known sinusoidal shear-stress perturbations generated via acoustic plane-wave excitation.[48,49] The sensor exhibited ≈40 dB/decade roll-off with a corner frequency of ≈600 Hz, indicative of a highly damped 2nd-order system. The response of conventional uncompensated sensors has been modeled as a heated thin-film on a semi-infinite medium and results in a half-order system response.[50] The difference in response is explained by the presence of a sealed vacuum cavity that reduces the unsteady heat conduction into the substrate and limits the dissipation due to conduction losses into the thin membrane. The discovery of this unexpected dynamic behavior (2nd-order system) of an uncompensated MEMS hot-film sensor likely means that constant-temperature compensators do not produce a flat, zero-phase response as they were designed for a traditional hot film (1/2-order system) or hot wire (1st-order system). Several research groups have presented shear-stress spectra and/or statistical moments measured using vacuum cavity sensors compensated by constant temperature feedback circuits.[26,31,46] Clearly, the uncertainty of such data is unknown.

C. Indirect Optical Sensors

The operating principle of a laser-based wall shear-stress sensor is to measure the near wall velocity gradient directly via the Doppler shift of a set of diverging fringe patterns scattered in the viscous sublayer of a boundary layer (see Figure 11). Naqwi and Reynolds employed conventional optics to project and collect the incident and scattered light.[51] Fourguette et al. miniaturized this technique using optical MEMS (MOEMS) fabrication technology.[52] Experimental verification of this technique for a measurement volume centered at 66 μm above the surface possessing a vertical spatial resolution of 30 μm indicates a 99% accuracy up to $Re_x = 10^6$. Current limitations of this technique are cataloged in Naughton and Sheplak and include the following:[4]

1. Low data rate for unsteady measurements due to low near-wall seed density
2. Difficulties in fabricating a device that contains a probe volume entirely contained within the viscous sublayer at moderate and high Reynolds number turbulent boundary layers

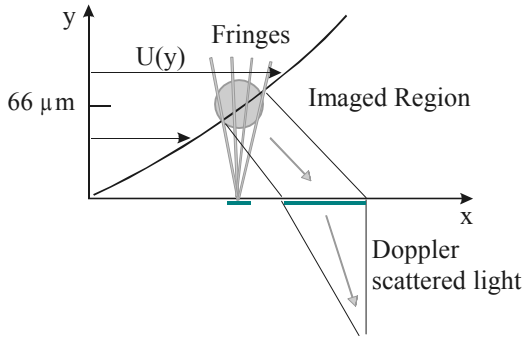

Figure 11 A schematic of the light scattered in diverging fringe patterns the MOEMS-based sensor.[31]

The latter difficulty has been addressed by employing a dual-probe sensor to obtain two measurement points, then using Spalding's formula as a curve fit to estimate the wall shear stress for $Re_x = 5x10^6$.[53]

D. Fence Sensors

Micro-fence sensors are a variation on a conventional surface fence measurement technique. For the convention implementation, the wall shear stress is inferred by playing a small fence within viscous sublayer of a turbulent boundary layer.[54] The static pressure drop across the upstream and downstream side of the fence is then related to the wall shear stress via a calibration curve. The microfence developed by Schober et al. replaces the surface pressure ports with a compliant cantilever beam possessing integrated piezoresistors to measure the pressure induced deflection as shown in Figure 12.[54] This device demonstrated the ability to obtain time-resolved measurements in separated flows. The device possesses moderate bandwidth (1 kHz) but has poor spatial resolution (5 mm). Schober et al. use an inverse linear filtering technique to extend the bandwidth, but the accuracy of such a practice given the asymmetric non-linear static response remains unresolved.

III. Conclusions

The MEMS community has produced a variety of direct and indirect shear-stress sensors. While much progress has been made, all of these devices are fairly immature and require further development to become reliable measurement tools possessing *quantifiable* uncertainties.

Floating element techniques appear to be best suited for obtaining quantitative, time-resolved data provided that a stable, low-noise transduction scheme can be developed that is immune to both EMI and transverse motions. From a packaging perspective, the sensor system must possess backside electrical or optical interconnects to provide a truly flush-mounted device. The robustness of the sensors to debris must also be addressed by covering the sensor gaps.

The extension of thermal sensors to quantitative turbulence measurements is non-trivial for several reasons. First, correcting for static temperature drifts remains an unresolved issue. Beyond the temperature

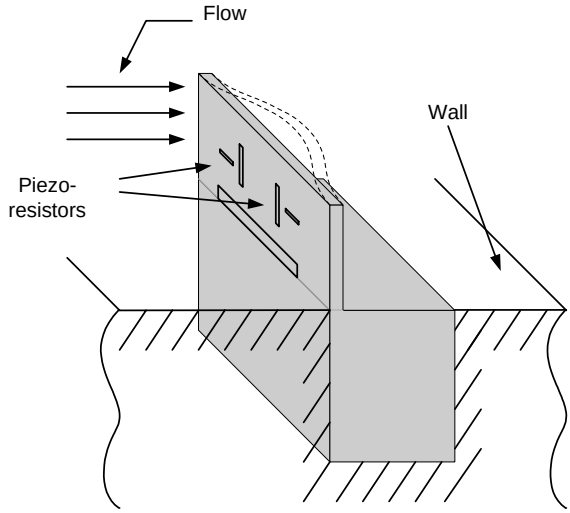

Figure 12 A schematic of the MEMS-based surface fence.[54]

issue is the requirement that the open loop dynamic response of the device be known to enable the design of suitable feedback compensation electronics. The complex conjugated heat-transfer interactions between the sensor and the supporting substrate/membrane results in an unknown frequency response function for the uncompensated sensor. Therefore, an in-situ dynamic calibration is required to determine the frequency response function of these devices. Until the these issues are resolved, MEMS based thermal shear stress sensors will not realize their full potential as quantitative devices.

The MOEMS-based technique is the most mature of the reviewed devices. It is very accurate provided that the probe volume lies within the viscous sublayer. The extension of this device to higher Reynolds numbers requires that this volume be reduced in size and brought nearer to the wall. The promise of time-resolved data seems unlikely because of near-wall seeding difficulties.

The micro-surface fence possesses similar limitations as the MOEMS-based technique at higher Reynolds numbers. The spatial resolution limitations are similar to the conventional floating element sensor tradeoff between small size and the ability to measure small forces. The asymmetric nonlinear static response also requires further study to determine the associated uncertainties.

Acknowledgments

The authors express their gratitude to Air Force Office of Scientific Research (F4962-97-1-0507), National Science Foundation (CTS-04352835), NASA-LaRC (NAG-1-2133), and NASA-KSC (NAG-10-316) for supporting the UF shear-stress sensor development. They also thank Brian Homeijer and Tai-An Chen for their illustrations.

References

1. Winter, K.G., "An Outline of the Techniques Available for the Measurement of Skin Friction in Turbulent Boundary Layers," *Progress in the Aeronautical Sciences,* Vol. 18, 1977, pp. 1-57.
2. Haritonidis, J.H., "The Measurement of Wall Shear Stress," *Advances in Fluid Mechanics Measurements*, Ed. by M. Gad-El-Hak, Springer-Verlag, 1989, pp. 229-261.
3. Fernholtz, H.H., Janke, G., Schober, M., Wagner, P.M., and Warnack, D., "New Developments and Applications of Skin-Friction Measuring Techniques" *Meas. Sci. Technol.*, Vol. 7, 1996, pp. 1396–1409.
4. Naughton, J. and Sheplak, M, "Modern Developments in Shear-Stress Measurement," *Prog. Aero. Sci.,* Vol. 38, 2002, pp. 515-570.
5. Tennekes, H. and Lumley, J.L., A First Course in Turbulence, MIT Press, Cambridge, MA, Chapter 1, 1972.
6. Alfredsson, P.H., Johansson, A.V., Haritonidis, J.H., and Ecklemann, H., "The Fluctuating Wall-Shear Stress and the Velocity Field in the Viscous Sublayer," *Phys. Fluids,* 31 (5), May 1998, pp. 1026-1033.
7. Madou, M., Fundamentals of Microfabrication, CRC Press, New York, 1997.
8. Löfdahl, L. and Gad-el-Hak, M., "MEMS-Based Pressure and Shear Stress Sensors for Turbulent Flows, "*Meas. Sci. Technol.* Vol. 10, 1999, pp. 665-686.
9. Schmidt MA, Howe RT, Senturia SD, Haritonidis JH, "Design and Calibration of a Microfabricated Floating-Element Shear-Stress Sensor," *Trans. Electron Dev.,* ED-35, pp. 750-757, (1988).
10. Padmanabhan, A., Sheplak, M., Breuer, K.S., and Schmidt, M.A., "Micromachined Sensors for Static and Dynamic Shear Stress Measurements in Aerodynamic Flows," *Technical Digest*, Transducers '97, Chicago, IL, 1997, pp. 137-140.
11. Hinze, J.O., Turbulence, 2nd ed., McGraw-Hill, New York, 1975.
12. Ng K, Shajii J, Schmidt MA, "A Liquid Shear-Stress Sensor Using Wafer-Bonding Technology," *J. MEMS* Vol. 1, 1992 , pp. 89-94.
13. Goldberg HD, Breuer KS, Schmidt MA, "A Silicon Wafer-Bonding Technology for Microfabricated Shear-Stress Sensors with Backside Contacts," *Tech. Dig., Solid-State Sensor and Actuator Workshop,* 1994, pp. 111-115.
14. Padmanabhan A, Goldberg HD, Schmidt MA, Breuer KS, "A Wafer-Bonded Floating-Element Shear-Stress Microsensor with Optical Position Sensing by Photodiodes," *J. MEMS,* Vol. 5, 1996, 307-315.
15. Sheplak, M., Padmanabhan, A., Schmidt, M.A., and Breuer, K.S., "Dynamic Calibration of a Shear Stress Sensor using Stokes Layer Excitation," *AIAA Journal,* Vol. 39, No.5, 2001, pp. 819-823.
16. Pan, T, Hyman D, Mehregany M, Reshotko E, and Garverick *S,* "Microfabricated Shear Stress Sensors, Part 1: Design and Fabrication," *AIAA J*, Vol. 37,1999, pp. 66-72.
17. Hyman, D., Pan, T., Reshotko, E, and Mehregany, M., "Microfabricated Shear Stress Sensors, Part 2: Testing and Calibration," *AIAA J*, Vol. 37, No.1, 1999, pp. 73-78.

18. Zhe, J, Farmer, K.R., and Modi, V., "A MEMS Device for Measurement of Skin Friction Using Capacitance Sensing," *Proc. of IEEE MEMS 01*, 2001, pp. 4-7.
19. Tseng, F.-G. and Lin C.-J., "Polymer MEMS-Based Fabry–Perot Shear Stress Sensor," *IEEE Sensors J*., Vol. 3, No. 6, 2003, pp. 812-817.
20. Horowitz, S., Chen, T., Chandrasekaran, V., Tedjojuwono, K., Nishida, T., Cattafesta, L., and Sheplak, M., "A Micromachined Geometric Moire Interferometric Floating-Element Shear Stress Sensor," AIAA Paper 2004-1042, 42nd Aerospace Sciences Meeting and Exhibit, Reno, NV, January 2004.
21. Horowitz, S., Chen, T., Chandrasekaran, V., Tedjojuwono, K., Nishida, T., Cattafesta, L., and Sheplak, M., "A Wafer-Bonded, Floating Element Shear-Stress Sensor Using a Geometric Moiré Optical Transduction Technique," *Tech. Dig., Solid-State Sensor and Actuator Workshop,* 2004, pp. 13-18.
22. Liu, C., Tai, Y.C., Huang, J., and Ho, C.M., "Surface Micromachined Thermal Shear Stress Sensor," Proceedings, The ASME Symposium on Application of Microfabrication to Fluid Mechanics, ASME Winter Annual Meeting, Chicago, 1994, pp. 9-15.
23. Ho, C-M. and Tai, Y-C, "Microelectromechanical Systems (MEMS) and Fluid Flows," *Annu. Rev. Fluid Mech.,* Vol. 30, 1998, 579-612.
24. Liu C, Huang C-B, Zhu Z, Jiang F, Tung S, Tai Y-C, and Ho C-M., "A Micromachined Flow Shear-Stress Sensor Based on Thermal Transfer Principles," *J. MEMS,* Vol. 8, pp. 90-99, (1999).
25. Wang, X-Q, Han, Z., Jiang, F., Tsao, T, Lin, Q., Tai, Y-C, Koosh, V., Goodman, R., Lew, J., and Ho, C-M., "A Fully Integrated Shear-Stress Sensor," *Proc. Transducers 99,* pp. 1074-1077.
26. Kimura, M. Tung, S., Lew, J., Ho, C-M., Jiang, F., and Tai, Y-C, "Measurements of Wall Shear Stress of a Turbulent Boundary Layer Using a Micro-Shear-Stress Imaging Chip, " *Fluid Dynamics Research*, Vol. 24, 1999, pp. 329-342.
27. Cain, A., Chandrasekaran, V., Nishida, T, and Sheplak, "Development of a Wafer-Bonded, Silicon Nitride Membrane Thermal Shear-Stress Sensor with Platinum Sensing Element," Technical Digest, Solid-State Sensor and Actuator Workshop, 2000, pp. 300-303.
28. Sheplak M, Chandrasekaran V, Cain A, Nishida T, Cattafesta L. , "Characterization of a Micromachined Thermal Shear Stress Sensor," *AIAA J*, Vol. 40, No. 6, pp. 1099-1104, (2002).
29. Appukuttan, A., Shyy, W., Sheplak, M., and Cattafesta, L., "Mixed Convection Induced by MEMS-Based Thermal Shear Stress Sensors," *Numerical Heat Transfer-A,* Vol. 43, No. 3, 2003, pp. 283-305
30. Yoshino, T., Suzuki, Y., Kasagi, N., and Kamiunten, S., "Optimum Design of Micro Thermal Flow Sensor and Its Evaluation in Wall Shear Stress Measurement, " Int. Conf. MEMS'03, 2003, pp. 193-196.
31. Yoshino, T., Suzuki, Y., Kasagi, N., and Kamiunten, S., "Assessment of the Wall Shear Stress Measurement with Arrayed Micro Hot-film Sensors in a Turbulent Channel Flow," Proc. 2nd Int. Symp. Turbulence and Shear Flow Phenomena, Stockholm, (2001), Vol. 2, pp. 153-158.
32. Bertlerud, A. , "Transition on a Three-Element High Lift Configuration at High Reynolds Numbers, " *AIAA Aerospace Sciences Meeting & Exhibit, 36th*, Reno, NV, Jan. 12-15, 1998, AIAA Paper 98-0703.
33. McGinley, C.B., Anders, J.B., Spaid, F.W., Measurements of Reynolds Stress Profiles on a High-Lift Airfoil, AIAA, Applied Aerodynamics Conference, 16th, Albuquerque, NM, June 15-18, 1998, AIAA Paper 98-2620.
34. Bellhouse, B.J., Schultz, D.L. " Determination of Mean and Dynamic Skin Friction, Separation and Transition in Low-Speed Flow with a Thin-Film Heated Element", *Journal of Fluid Mechanics*, Vol. 24, Feb. 1966, pp. 379-400.
35. Mathews, J. "The Theory and Application of Heated Films For The Measurement of Skin Friction in Incompressible Flows," Ph.D Dissertation, Cranfield Institute of Technology College of Aeronautics, Sept. 1985.
36. Cousteix, J., Juillen, J.-C., "Hot wire Gauges for Skin Friction Measurement (Design, Calibration, Applications)," *La Recherche Aerospatiale (English Edition),* No. 3, 1982, pp. 63-74.
37. Bruun, H.H., *Hot-wire Anemometry, Principles and Signal Analysis*, Oxford University Press Inc., New York, 1995, pp. 215-219.
38. Bearman, P. W., "Corrections for the Effect of Ambient Temperature Drift on Hotwire Measurements in Incompressible Flow," *DISA Information*, No. 2, May 1971, pp.25-30.
39. Kanevce, G and Oka, S., "Correcting Hot-wire Readings for Influence of Fluid Temperature Variations" *DISA Information*, No. 15, Oct. 1973, pp. 21-24.
40. Cimbala, J. M., Park, W. J., "A Direct Hot-Wire Calibration Technique to Account for Ambient Temperature Drift in Incompressible Flow," *Experiments In Fluids*, Vol. 8, No. 5, 1990, pp. 299, 300.

41. Papanicolaou, P.N., Papaspyros, J.N.E., Kastrinakis, E.G., Nychas, S.G., "A Fast Digital Technique for Calibration of Hot-Wires over a Wide Temperature Range," *Measurement Science & Technology*, Vol. 8, No.11, Nov. 1997 pp.1363-1366.
42. Nagaoka Y., Alexander H.G., Liu W, Ho C.M., " Shear Stress Measurements On An Airfoil Surface Using Micro-Machined Sensors," *JSME International Journal Series B-Fluids and Thermal Engineering,* Vol. 40, No. 2, May 1997, pp. 265-272 .
43. Jiang, F., Tai, Y. C., Gupta, B., Goodman, R., Tung, S., Huang J, Ho C. M. "A Surface-Micromachined Shear-Stress Imager," *Proc. IEEE Micro Electro Mechanical Systems Meeting,* San Diego*, CA,* 1996, pp. 110–115.
44. Huang, J.B., Jiang, F. K., Tai, Y.C., Ho, C.M., "A Micro-Electro-Mechanical-System-Based Thermal Shear-Stress Sensor with Self-Frequency Compensation," *Measurement Science and Technology,* Vol. 10, No. 8, Aug. 1999, pp. 687-696.
45. Ruedi J.D., Nagib H., Osterlund J., Monkewitz P. A., "Evaluation of Three Techniques For Wall-Shear Measurements in Three-Dimensional Flows," *Experiments in Fluids,* Vol. 35, No. 5, Nov. 2003, pp. 389-396.
46. Ruedi, J.D., Nagib, H., Österlund, J., Monkewitz, P. A., "Unsteady Wall-Shear Measurements in Turbulent Boundary Layers Using MEMS," *Experiments in Fluids*, Vol. 36, No. 3, Mar. 2004, pp. 393-398.
47. Lofdahl L, Chernoray V, Haasl S, Stemme G, Sen M, "Characteristics of a Hot-Wire Microsensor for Time-Dependent Wall Shear Stress Measurements", *Experiments In Fluids,* Vol. 35, No. 3, Sept. 2003, pp. 240-251.
48. Sheplak, M., Padmanabhan, A., Schmidt, M.A., and Breuer, K.S., "Dynamic Calibration of a Shear Stress Sensor using Stokes Layer Excitation", *AIAA Journal*, Vol. 39, No.5, May 2001, pp. 819-823.
49. Chandrasekaran, V., Cain, A., Nishida, T., and Sheplak, M., "Dynamic Calibration Technique for Thermal Shear Stress Sensors with Variable Mean Flow," AIAA Paper 2000-0508, 2000.
50. Ling, S.C. and Hubbard, P.G., "The Hot-Film Anemometer: A New Device for Fluid Mechanics Research," *J. Aero. Sci.*, Vol. 23, 1956, pp. 890-891.
51. Naqwi, A.A. and Reynolds, W.C., "Dual Cylindrical Wave Laser-Doppler Method for Measurement of Skin Friction in Fluid Flow," Report No. TF-28, Stanford University, 1987.
52. Fourguette, D., Modarress, D., Taugwalder, F, Wilson, D., Koochesfahani, M, and Gharib, M., "Miniature and MOEMS Flow Sensors," AIAA Paper 2001-2982, 2001.
53. Fourguette, D., Modarress, Wilson, D. D., Koochesfahani, M, and Gharib, M, "An Optical MEMS-Based Shear Stress Sensor for High Reynolds Number Applications," AIAA Paper 2003-0742, 2003.
54. Schober, M., Obermeier, E., Pirskawetz, S. and Fernholz, H.-H. " A MEMS Skin-Friction Sensor for Time-resolved Measurements in Separated Rlows," *Exp. in Fluids*, Vol. 36, 2004, pp. 593–599.